Laosuwan, T., Itsarawisuti, J., Uttaruk, Y., Sangpradid, S., Rotjanakusol, T., Peebkhunthod, T. (2025). Urban tree carbon stock assessment based on remote sensing and field inventory data. Agriculture and Forestry, 71 (4): 17-35. https://doi:10.17707/AgricultForest.71.4.02

DOI: 10.17707/AgricultForest.71.4.02

Teerawong LAOSUWAN[1,2 3] , Jumpol ITSARAWISUT[1,2]*, Yannawut UTTARUK[3,4], Satith SANGPRADID[4,5], Tanutdech ROTJANAKUSOL[1,2,3,] Thanakrizt PEEBKHUNTHOD[6]

URBAN TREE CARBON STOCK ASSESSMENT BASED ON REMOTE SENSING AND FIELD INVENTORY DATA

SUMMARY

The increasing concentration of CO_2 in the atmosphere is one of the causes that has lead to what we define as global warming with dramatic events on ecosystems, biodiversity and human life. An accurate prediction of aboveground biomass (AGB) and carbon stock is crucial for the assessment of forest and urban trees' contributions to climate game. The objective of this study was to establish a reliable way to estimate aboveground biomass and potential carbon stock by integrating remote sensing methods with ground-based measurements. The procedure consisted of the following three major steps: (1) calculation of NDVI, GNDVI and SAVI; (2) systematic sampling of field plots using species distribution by biomass and carbon quantification through allometric equations according to the species; and (3) exponential regression between biomass vs vegetation indices. Results indicated that GNDVI has the maximum correlation with biomass in comparison with NDVI, and SAVI. When extrapolated, GNDVI model predicted 2798.23 and 1315.17 tons of above ground biomass and carbon respectively. In the field, biomass and carbon was measured as 4,650.75 tons and 2,185.85 tons respectively. These results also highlight the significance of integrating remote sensing and field data for precise estimation of biomass and

[1] Teerawong Laosuwan, Jumpol Itsarawisut (*corresponding author: drjumpol.i@gmail.com), Tanutdech Rotjanakusol, Department of Physics, Faculty of Science, Mahasarakham University, Maha Sarakham, 44150.THAILAND;

[2] Teerawong Laosuwan, Jumpol Itsarawisut, Tanutdech Rotjanakusol, Space Technology and Geoinformatics Research Unit, Faculty of Science, Mahasarakham University, Maha Sarakham, 44150, THAILAND.

[3] Teerawong Laosuwan, Yannawut Uttaruk, Tanutdech Rotjanakusol, Greenhouse Gas Research Center and Operations, Faculty of Science, Mahasarakham University, Maha Sarakham, THAILAND.

[4] Yannawut Uttaruk, Satith Sangpradid, Department of Biology, Faculty of Science, Mahasarakham University, Maha Sarakham, 44150.THAILAND

[5] Satith Sangpradid, Department of Geoinformatics, Faculty of Informatics, Mahasarakham University, Kantarawichai, Mahasarakham 44150, THAILAND

[6] Thanakrizt Peebkhunthod, Mahasarakham University Demonstration School, Mahasarakham University, Kantarawichai, Maha SaraKham, 44150, THAILAND

Notes: The authors declare that they have no conflicts of interest. Authorship Form signed online.

Recieved:07/09/2025 *Accepted:25/10/2025*

carbon, providing useful information even for resource management, urban green planning and global climate change countermeasures such as a carbon credit program.

Keywords: remote sensing, urban forest, aboveground biomass, carbon sequestration, allometric equations, carbon credit, net zero

INTRODUCTION

Global warming and climate change are now great international concerns. One of the major contributors to these issues, is the rise in greenhouse gases (GHG), specifically carbon dioxide (CO_2), released into the atmosphere from human activities like industrial processes, transportation and everyday energy use (Uttaruk and Laosuwan, 2020). The effects of the change in climate are now becoming increasingly evident across the globe (Angkahad *et al*., 2025a). Biodiversity is also affected by increasing global temperature, which has led to the adaption of many species into new areas (Muluneh, 2021). Others will go extinct if they don't evolve fast enough. Further, many ecosystems are deteriorating, causing imbalances in the natural elements that sustain life. These secondary effects reach outside of the natural environment and are beginning to impact human living standards from local issues up to a global level.

Farmers attempt to adapt their farming practices to changing climate conditions, such as unpredictable rainfall and droughts that reduce crop yields (Semosa, 2025). Public health is also under threat, with communities experiencing increases in heat-related illnesses and greater exposure to air pollution (Ofremu *et al*., 2025). In this regard, the ecosystem services (involving urban trees) have been referred to one of the key strategies for both climate change adaption and mitigation (Rahim *et al*., 2024). Atmospheric CO_2 is captured by trees and stored as organic carbon in their AGB (Laosuwan *et al*., 2025a; Uttaruk *et al.,* 2024). In addition to carbon sequestration, they serve as a critical mitigation against heat-related urban heat islands, air pollutions via filtration and therapeutic green spaces that benefit both physical and psychological health for citizens living in the city (Wolf *et al.,* 2020).

Aboveground biomass (AGB) is a principle parameter commonly used to estimate the carbon sequestered in vegetation because it is directly related to carbon stored in different components of a tree including tree trunks, branches, leaves and roots (Laosuwan *et al.,* 2025b; Saengpradit *et al.,* 2024; Vattanavongsiri *et al.,* 2023). The estimation of AGB in various zones is valuable tool for sustainable natural resource management, urban planning and environmental restoration. In general, the estimation of AGB is based on measurements of the physical characteristics of trees such as tree height, DBH and crown size (Bhebhe *et al.,* 2025; Liu *et al*., 2024a). These measurements can be employed in allometric equations to estimate aboveground biomass and carbon stocks precisely (Laosuwan *et al*., 2023).

Environmental data, in particular for biomass and carbon studies, can be effectively gathered and analyzed by remote sensing technology. Remote sensing allows for fast and reliable results since it minimizes fieldwork (Lamenkova, 2024) as well as time and labor demands, by making images coming from satellite or aerial available (Roy *et al*., 2016). One of their main advantages is the long-term monitoring of biomass changes by which researchers can assess the effects of land use, resource management practices and environmental policies (Dhiman and Kumar, 2024; Castillo *et al.,* 2017). As a result, remote sensing has become one of the pivotal tools for progressive and sustainable resources management and supporting scientific based decision-makings (Angkahad *et al.,* 2025b).

In urban environments, predicting AGB and carbon storage highlights the significant contributions of urban ecosystems to climate change abatement (Aabeyir *et al*., 2020). The expansion and maintenance of urban green spaces not only absorbs atmospheric CO_2 but also helps reduce the urban heat island effect, improve local air quality, and increase physical and psychological welfare for residents (Xiao *et al.,* 2022). Thus, bridging remote sensing approaches with urban forestry work provides a powerful avenue for greener and more climate-resilient city design (Wavrek *et al*., 2023). Because the carbon stored in trees is closely related to their biomass, an accurate prediction would have to consider structural parameters such as tree height, diameter at breast height and crown width. These parameters are frequently used in species-specific allometric equations, and are predictive of aboveground biomass and carbon estimates (e.g., Ngomanda *et al*., 2014; Van Breugel *et al*., 2011). The knowledge gained from such research is essential for the development of local and national climate policy, for CO_2 mitigation strategies, and adaptive planning with future climate scenarios (IPCC, 2022). Given these challenges and opportunities, there is a clear need for more reliable methods of assessment. Accordingly, the present study proposes an integrated approach that combines remote sensing data with field measurements to improve the accuracy of AGB and carbon stock estimation in urban trees.

MATERIAL AND METHODS

Study Area

The study of carbon storage from urban trees was conducted in the campus of Mahasarakham University (Figure 1), Talad Sub-district, Mueang Maha Sarakham District, Maha Sarakham Province, Thailand. The site has coordinates of E 316471.52 and N 1791741.78 and Maha Sarakham is in predominating flat plain with slight undulating hills, the elevation ranges from 130 to 230 meters above sea level. The climate of the area is tropical monsoon type, with strong influences from the southwest monsoon wind flow from Indian Ocean in summer season giving distinct warm wet and dry season. This region has an average annual temperature of 27.4 °C, and the mean monthly temperatures vary from around 22.4 °C during the coldest months to even 33.7 °C in the hottest months.

April is usually the full-swing summer and the hottest month of the year.

Other than the climate, the campus of Mahasarakham University is endowed with mixed land use such as academic buildings, open green fields and random tree clusters to enhance ecological stability of the campus. These downtown trees help provide cover for sidewalks, they reduce the temperature of the walking surfaces and they improve the quality of air that students and workers breathe. This green envelope of the campus is an ideal living laboratory for research in carbon sequestration, urban forestry and sustainable environmental management.

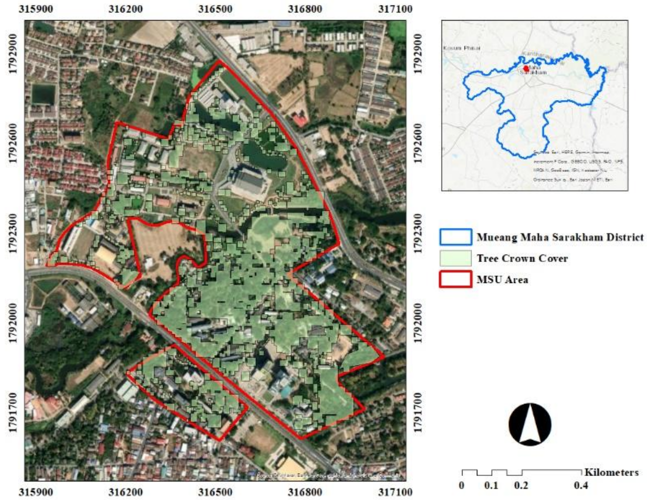

Figure 1. Urban trees within the campus of Mahasarakham University

Tree Physical Data Analysis

The field survey in this research was conducted to collect information on tree species and physical attributes of each individual specimens sample in the study site. This measurement was performed in 30 sample plots of 20 m x 20 m each. Within each plot, measurements were obtained from all trees >4.5 cm DBH. Tree diameter at breast height (DBH) was measured with a diameter type and tree height (H) was recorded with a laser rangefinder. These two variables, DBH and H, are the basic measures of tree growth and form.

The measurements obtained were subsequently used in an allometric equation to convert DBH and H into aboveground biomass (AGB) values, representing the amount of biomass stored in each tree (Equation 1) (Ogawa *et al*., 1965). Once AGB values were determined, they were applied to a carbon conversion equation (Equation 2) to estimate the quantity of carbon sequestered in the trees (Intergovernmental Panel on Climate Change, 2006). This approach, combining allometric equations for biomass and carbon estimation, is a key step in evaluating the environmental value of trees at the local scale. Moreover, the resulting data provide a scientific foundation for academic research and can inform effective planning and management of urban green spaces.

$$
\begin{aligned}
W_S &= 0.0396(D^2H)^{0.933} \\
W_B &= 0.00349(D^2H)^{1.030} \\
W_L &= \left(\frac{28}{W_S + W_B} + 0.025\right)^{-1} \\
W_T &= W_S + W_B + W_L
\end{aligned}
\qquad (1)
$$

D denotes diameter at breast height (cm), H represents tree height (m), WS indicates stem biomass (t ha^{-1}), WB represents branch biomass (t ha^{-1}), WL denotes leaf biomass (t ha^{-1}), and WT refers to total aboveground biomass (t ha^{-1}).

$$C_j = W_{tc} \times FC \tag{2}$$

C_j represents the carbon storage potential of an individual tree (kg), W_tc denotes its aboveground biomass (kg), and FC is the carbon fraction of biomass, which is assumed to be constant at 0.47.

Satellite Image Data Processing

Sentinel-2 satellite images were used as a primary source of data for the assessment of vegetation conditions within the study area. In this analysis, three commonly applied vegetation indices, namely NDVI (normalized difference vegetation index) (Tucker 1979), GNDVI (green normalized difference vegetation index) (Gitelson *et al.*, 1996) and SAVI (soil adjusted vegetation index) (Huete 1988), were derived as described in Equation 3–5. When the vegetation index values were obtained, they were used to calculate FC (Fractional Green Vegetation Cover) in a second step according to Equation 6, to transform the index values into physical takes on surface fraction of green canopy. The selection of these indices is important due to the information they have embedded about vegetation cover, phenological stages and general condition of plants within our study area, which in combination provides a sound basis for conducting spatial analysis to estimate aboveground biomass and carbon stocks at the landscape level.

$$NDVI = \frac{NIR - RED}{NIR + RED} \tag{3}$$

The Normalized Difference Vegetation Index (NDVI) is a simple yet powerful indicator of green vegetation, comparing near-infrared reflectance with red-light absorption by chlorophyll. NDVI values range from −1 to 1, with negative values typically indicating water bodies, values near zero (−0.1 to 0.1) representing barren areas such as rock, sand, or snow, moderate positive values (≈0.2–0.4) indicating shrubs and grasslands, and values approaching 1 corresponding to dense temperate and tropical forests.

$$GNDVI = \frac{NIR - GREEN}{NIR + GREEN} \tag{4}$$

The Green Normalized Difference Vegetation Index (GNDVI) is widely used to assess plant greenness and photosynthetic activity, particularly for evaluating water and nitrogen uptake within the crop canopy. Its values range from −1 to 1, with negative values (−1 to 0) indicating water or bare soil. GNDVI is especially useful during the intermediate and late stages of crop growth.

$$SAVI = \frac{(NIR - RED) \times (1 + L)}{(NIR + RED + L)} \tag{5}$$

NIR denotes the reflectance in the near-infrared band, Red represents the reflectance in the red band, and L is the soil brightness correction factor that reduces the influence of soil background on the vegetation signal. The value of L generally ranges from 0 for areas with very dense vegetation to 1 for bare soil, with 0.5 commonly applied in regions with moderate vegetation cover.

$$FC = \frac{Index - Index_{soil}}{Index_{forest} - Index_{soil}} \tag{6}$$

Index refers to the vegetation index values used for analysis. Indexforest represents the vegetation index values of areas with the densest vegetation cover, while IndexSoil represents the vegetation index values of areas without vegetation (bare soil).

Correlation Analysis

The relationship between Fractional Green Vegetation Cover (FC) and aboveground biomass (AGB) density was evaluated using an exponential regression model, which has proven to be effective for estimating biomass from Sentinel-2 satellite data. The general form of the regression model is expressed in Equation 7.

$$AGB = a \times b^{e \times FC} \tag{7}$$

a represents the intercept of the regression curve, and b is the regression coefficient that determines the rate of biomass increase as FC rises. The analysis revealed that AGB increases exponentially with FC, confirming a strong positive relationship between vegetation cover and biomass accumulation in the study area.

Model Accuracy Assessment Using Root Mean Square Error (RMSE)

The accuracy of the model in estimation of AGB density was examined by comparing predicted values with the field-measured observations. The model evaluation criterion was the Root Mean Square Error (RMSE), which is defined as in Equation 8. RMSE is measured from the observed and predicted values, where each difference (observed – predicted value) is squared; then an average of the squared differences is computed, and finally you square root to get back to the original range.

RMSE can be used to quantify the degree of prediction error, with lower

values indicating the model's performance and hence lower deviation between prediction and measurements. In the present study where satellite derived VIs were employed to estimate AGB, RMSE offered an important criterion for validating model robustness. Additionally, RMSE can be used as a diagnostic measure for analyzing potential error sources and model improvement, thus helping to secure biomass assessments in other landscape types.

$$RMSE = \sqrt{\Sigma\ (Pi\ -\ Oi)^2\ /\ n} \tag{8}$$

P_i represents the predicted biomass value derived from the vegetation index, O_i denotes the observed biomass value obtained from field measurements, and n indicates the total number of samples.

RESULTS AND DISCUSSION

This section presents the findings of the study, beginning with the results of field data collection and the calculation of aboveground biomass (AGB) and carbon stock, followed by the analysis of vegetation indices, model development, and accuracy assessment. The discussion integrates these results to highlight key patterns, interpret their ecological significance, and evaluate the potential of remote sensing for large-scale biomass and carbon estimation.

Results of Tree Physical Data Processing

Field surveys were conducted from 4 to 5 October 2024, coinciding with the end of the rainy season—an ideal period for data collection due to favorable weather that enabled efficient and uninterrupted measurements.

Table 1. Results of Tree Physical Data Processing

Plot	Mean DBH (cm)	Mean Height (m)	Branch Biomass (kg)	Stem Biomass (kg)	Leaf Biomass (kg)	Total AGB (kg)	Total AGB (t/400 m²)	Total AGB (t/ha)
01	21.23	7.23	235.08	1,156.81	49.72	1,441.61	1.44	36.04
02	21.69	5.43	1,079.90	3,949.66	179.64	5,209.20	5.21	130.23
03	22.36	8.23	271.52	1,338.01	57.49	1,667.02	1.67	41.68
04	19.78	7.94	310.43	1,501.53	64.73	1,876.69	1.88	46.92
05	38.48	12.00	1,439.85	5,754.56	256.95	7,451.36	7.45	186.28
06	35.65	10.67	476.37	2,043.86	90.01	2,610.25	2.61	65.26
07	37.40	14.13	1,104.23	4,421.06	197.34	5,722.63	5.72	143.07
08	28.46	10.60	489.38	2,206.36	96.29	2,792.02	2.79	69.80
09	67.48	21.75	2,032.66	7,474.00	339.53	9,846.19	9.85	246.15
10	65.49	17.50	2,023.25	7,208.00	329.69	9,560.95	9.56	239.02
11	58.09	19.50	2,958.65	11,109.71	502.45	14,570.81	14.57	364.27
12	31.19	10.14	600.32	2,424.50	108.04	3,132.86	3.13	78.32
13	7.79	5.74	48.15	271.45	11.43	331.03	0.33	8.28
14	22.18	8.89	456.61	1,939.73	85.59	2,481.94	2.48	62.05
15	35.57	10.25	870.19	3,120.51	142.53	4,133.22	4.13	103.33
16	30.74	13.00	1,181.44	5,036.95	222.10	6,440.48	6.44	161.01
17	14.26	7.21	291.33	1,356.14	58.86	1,706.33	1.71	42.66
18	29.33	10.43	1,116.56	4,031.71	183.87	5,332.14	5.33	133.30
19	27.25	12.13	2,817.58	9,878.23	453.44	13,149.25	13.15	328.73
20	28.03	10.50	905.27	3,824.41	168.93	4,898.61	4.90	122.47
21	87.54	21.00	1,842.89	6,350.37	292.62	8,485.88	8.49	212.15
22	17.54	6.91	113.09	595.72	25.32	734.13	0.73	18.35
23	16.64	7.00	104.51	554.43	23.54	682.49	0.68	17.06
24	54.37	13.20	1,442.02	5,300.96	240.83	6,983.80	6.98	174.60
25	32.20	11.50	700.38	2,761.89	123.66	3,585.93	3.59	89.65
26	43.99	9.80	587.15	2,422.83	107.50	3,117.48	3.12	77.94
27	127.32	15.00	1,231.16	4,195.18	193.80	5,620.14	5.62	140.50
28	25.46	9.77	876.49	3,972.19	173.19	5,021.87	5.02	125.55
29	32.07	8.13	359.79	1,643.35	71.55	2,074.69	2.07	51.87
30	20.51	7.29	213.80	1,085.46	46.41	1,345.68	1.35	33.64

In each sample plot, all trees were measured for diameter at breast height (DBH) and total height (H), and the geographic coordinates of each plot were recorded using a GPS device to ensure spatial accuracy. The information showed great mutation of tree features among the plots. AGB (aboveground biomass) was estimated employing species-specific allometric equations using DBH and height values, shown in Table 1.

The total AGB of the study area is estimated to be 4,650.75 tons which means that there are approximately 2,185.85 tons of carbon in stock. Positive linear relationship was found between biomass accumulator, mean DBH and tree height. For instance, Plots 11 and 27 with mean DBH of 58.09 cm and 127.32 cm had total biomass of 14,570.81 kg and 5620.14 kg respectively. Plots 21 and 19 also had high biomass values at 8,485.88 kg and 13,149.25 kg respectively. In tons per hectare (t/ha), Plot 11 had the highest biomass density with 364.27 t/ha, whereas plot 13 recorded the lowest with only 8.28 t/ha of biomass.

These findings may reflect the differences in the structure of forest stands of the study region, being mixed species and uneven aged forests where competition for light, nutrients and space could cause to vary growth patterns. The high positive correlation between DBH and biomass is consistent with studies of the Chave *et al*. (2014) and Saatchi *et al.* (2021), indicating that DBH is a good predictor of AGB.

Very high biomass density in Plot 11 likely indicates mature and highly stocked trees with high potential for carbon sequestration, while low biomass density in Plot13 may be due to younger stands or lower density of trees, or recent disturbances such as thinning, natural mortality. That variation really drive home the value of spatially explicit measurements and stratified sampling in landscape level biomass estimation. Management wise, conservation values of high biomass plots are important due to their significant impact on carbon sequestration and the low biomass areas may be targeted for rehabilitation or enrichment planting. Combined, this information forms the basis for informed decisions in forest management and climate mitigation plans.

Results of Satellite Image Analysis

Satellite imagery from Sentinel-2 was utilized to evaluate vegetation indices across the Mahasarakham University area, providing a spatially explicit assessment of vegetation cover.

Three major indices were analyzed: NDVI (Normalized Difference Vegetation Index), GNDVI (Green Normalized Difference Vegetation Index), and SAVI (Soil-Adjusted Vegetation Index). The spatial patterns of these indices are illustrated in Figures 2 to 4, while their quantitative results are summarized in Table 2.

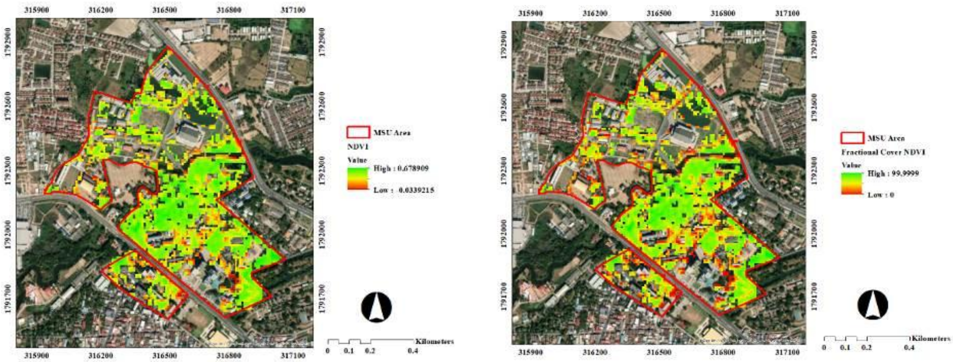

(a) (b)

Figure 2. (a) NDVI and (b) NDVI-derived Fractional Cover

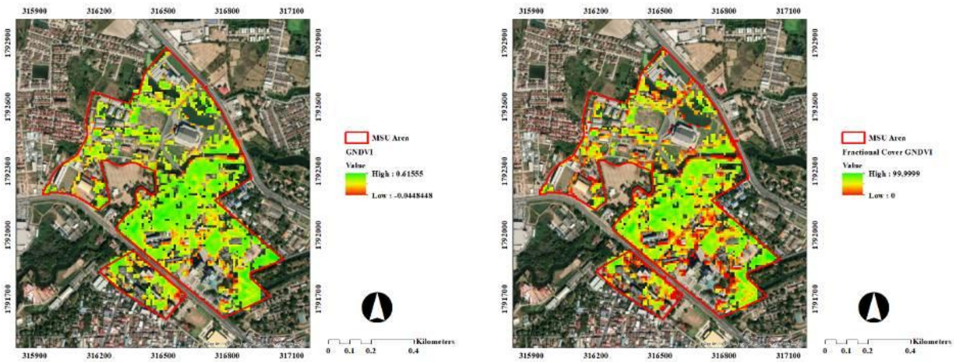

(a) (b)

Figure 3. (a) GNDVI and (b) GNDVI-derived Fractional Cover

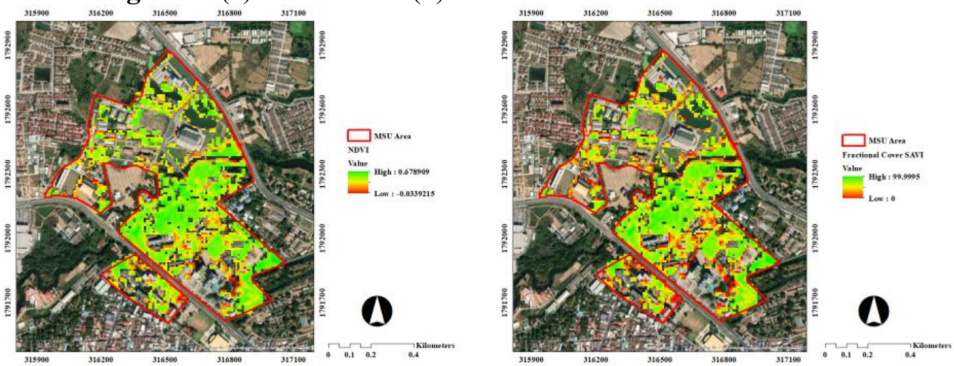

(a) (b)

Figure 4. (a) SAVI and (b) SAVI-derived Fractional Cover

Table 2. Fractional cover (%) derived from NDVI, GNDVI, and SAVI for the 30 sample plots

Plot	Fractional Cover (NDVI)	Fractional Cover (GNDVI)	Fractional Cover (SAVI)
1	61.15	48.62	61.15
2	69.17	58.15	69.17
3	75.91	65.02	75.91
4	73.43	64.29	73.43
5	67.17	55.91	67.17
6	75.20	66.05	75.20
7	64.97	51.54	64.97
8	57.75	45.84	57.75
9	77.01	69.48	77.00
10	73.56	64.39	73.56
11	58.19	46.17	58.19
12	72.68	63.83	72.68
13	84.75	77.76	84.75
14	75.60	68.10	75.59
15	76.37	67.60	76.37
16	41.81	32.78	41.81
17	82.75	74.08	82.74
18	79.07	71.33	79.07
19	83.27	76.89	83.27
20	80.99	73.68	80.99
21	42.54	32.93	42.53
22	84.97	74.92	84.96
23	87.21	83.20	87.21
24	66.64	56.92	66.64
25	45.91	37.92	45.91
26	69.82	61.19	69.82
27	82.61	72.73	82.61
28	74.54	67.04	74.54
29	63.15	49.50	63.15
30	74.29	67.07	74.28
Min	41.81	32.78	41.81
Max	87.21	83.20	87.21
Mean	70.75	61.50	70.75
SD	12.13	13.25	12.13

The NDVI values (Figure 2a) varied from −0.03 to 0.68, while the fractional green cover (Figure 2b) ranged between 0.00 % and 100.00 %. The GNDVI, in Figure 3a, was observed over the whole university surface area (in red) with similarly ranged (−0.03 to 0.68) values of fractional cover (Figure 3b) from 0.00 to 100.00 %. For SAVI, the numerical range was slightly wider (−0.05–1.02; Fig. 4a), though coded with values of fractional cover across an identical range from 0.00 to 100.000 %. Overall, these 3 indices provide a clear spatial delineation to green vegetation, representing the variability in canopy density across the landscape and forming an essential reference for further biomass and carbon sequestration investigations.

Fractional cover values are displayed for all 30 sample plots in Table 2 according to the three indices. NDVI varied from 41.81 % to 87.21 % with a mean of 70.75 % and a standard deviation (SD) of 12.13, signifying relatively dense vegetation in general condition for plots with moderate variability among the plots. GNDVI presented a mean of 61.50 % (range: 32.78–83.20 %, SD=13.25), slightly lower due to its strongest sensitivity to chlorophyll content. SAVI values were highly consistent with NDVI in minimum, maximum and mean values, which verified that SAVI was capable of adjusting the soil background effect and enhancing detection accuracy of vegetation in different soil environments.

At the plot-level, Plots 23, 19 and 22 showed the largest fractional cover across all indices reflect relatively vigorous growth of vegetation and a dense canopy cover; in contrast Plots 16 and 21 displayed the smallest values most likely due to site specific limitations i.e. drought stress, reduced stand density or soil infertility. The small differences between the indices illustrate the complementary nature of these: while NDVI gives an overall greenness measure, GNDVI picks up signals on chlorophyll concentration by leveraging information in the green band and SAVI accounts for soil influence - hence is particularly applicable in sparsely vegetated land surfaces. In general, simultaneous use of several vegetation indices leads to more thorough and reliable explanation of site properties. This integration will improve the empirical and spatial base of later modelling efforts to estimate aboveground biomass and carbon stock potential.

Analysis of the Relationship

This section analyzes the relationship between Fractional Vegetation Cover (FC) and Aboveground Biomass (AGB) using an exponential regression model, as presented in Figure 5. The results indicate that the GNDVI-based model provided the strongest relationship, achieving a coefficient of determination (R^2) of 0.7201. This finding demonstrates that variations in biomass can be reliably explained by FC values derived from GNDVI. The regression equation describing this relationship is expressed in Equation 9.

$$AGB=3.9972\times^{e0.0533\times FC}\ (R^2=0.7201) \quad (9)$$

where AGB is the estimated aboveground biomass (kg per plot) and FC is the fractional vegetation cover (%) derived from GNDVI.

The strength of GNDVI lies in its sensitivity to both the near-infrared and green spectral bands, which are closely associated with chlorophyll concentration and vegetation density. This spectral responsiveness allows GNDVI to capture vegetation greenness more precisely, resulting in a stronger and more consistent relationship between FC and AGB compared to other indices.

During the modeling process, the number of sample plots was reduced from 30 to 10 to enhance the robustness of the regression. This refinement was necessary because some plots exhibited irregular tree distribution patterns, particularly those with only a few large trees, which led to disproportionately high biomass values relative to their fractional cover. Such anomalies introduced bias and increased model error, thereby lowering the overall R^2.

By selecting plots with more homogeneous vegetation structure and clearer FC–AGB patterns, the reliability and predictive power of the model improved. Following this refinement, the R^2 value increased, confirming better model performance and reduced influence from outliers. Consequently, the final regression equation is more accurate and well-suited for predicting aboveground biomass in similar ecological settings.

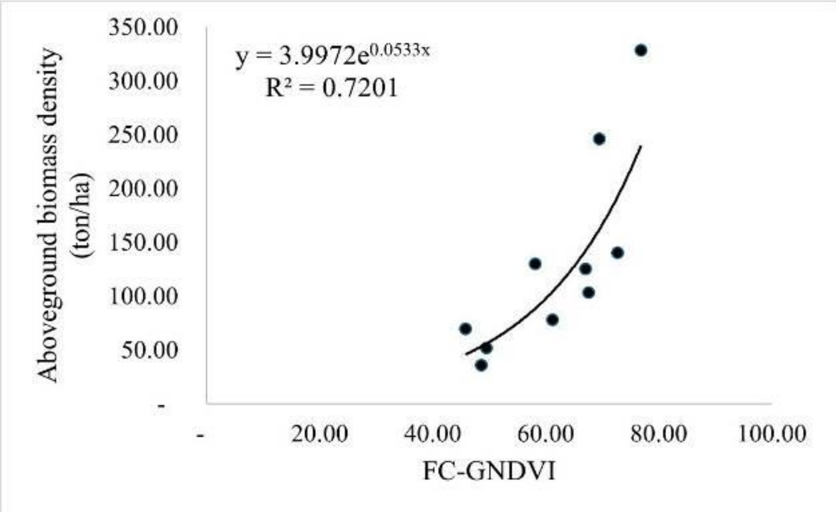

Figure 5. Relationship Between Fractional Cover and Aboveground Biomass

Spatial Assessment of Aboveground Biomass

The spatial estimation of aboveground biomass (AGB) and carbon storage across the study area was carried out using vegetation indices derived from Sentinel-2 imagery, applying the exponential regression model developed in the previous section. Biomass density (tons per hectare) was converted to biomass per pixel by multiplying the density values by the pixel area (100 m^2) and dividing by 10,000, thereby expressing the result in tons per pixel. The results of the spatial analysis were visualized in raster format, where each pixel represents an estimated AGB value, allowing a detailed examination of biomass distribution across the study area.

From NDVI (Figure 6a), biomass per pixel ranged from 0.01 to 6.54 tons, with a total AGB of 2,558.12 tons. GNDVI (Figure 6b) produced the highest biomass estimates, ranging from 0.04 to 8.25 tons per pixel and resulting in a total of 2,798.23 tons. SAVI (Figure 6c) resulted in values between 0.01 and 6.54 tons per pixel, corresponding to a total biomass of 2,558.02 tons. These findings provide a comprehensive picture of biomass accumulation, with GNDVI consistently yielding slightly higher estimates, indicating its greater sensitivity to vegetation density and chlorophyll concentration.

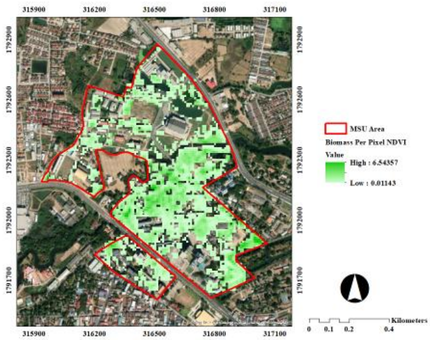

(a)

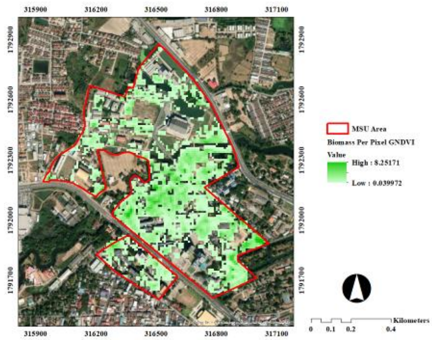

(b)

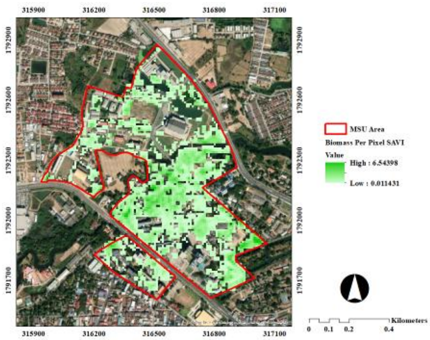

(c)

Figure 6. Biomass per pixel (a) NDVI, (b) GNDVI, and (c) SAVI

From NDVI (Figure 7a), biomass per pixel ranged from 0.01 to 6.54 tons, with a total AGB of 2,558.12 tons. GNDVI (Figure 7b) produced the highest biomass estimates, ranging from 0.04 to 8.25 tons per pixel and yielding a total of 2,798.23 tons. SAVI (Figure 7c) resulted in values between 0.01 and 6.54 tons per pixel, corresponding to a total biomass of 2,558.02 tons. These findings provide a comprehensive picture of biomass accumulation, with GNDVI consistently yielding slightly higher estimates, indicating its greater sensitivity to vegetation density and chlorophyll concentration.

The corresponding carbon stock estimates, derived from the same vegetation indices, exhibited a similar spatial pattern and are shown in Figures 7 (a)–(c). NDVI-based carbon values ranged from 0.0053721 to 3.07548 tons of carbon per 100 m^2 pixel, producing a total carbon stock of 1,202.316209 tons. GNDVI yielded the highest carbon estimates, with values ranging from 0.0187868 to 3.8783 tons of carbon per pixel and a total of 1,315.166321 tons. SAVI showed carbon values between 0.00537257 and 3.07567 tons, with a total of 1,202.271152 tons. These results confirm the spatial heterogeneity of carbon storage within the study area and emphasize the reliability of vegetation indices—particularly GNDVI—as effective tools for landscape-scale carbon stock assessment and mapping, providing essential information for precision forest management and climate-mitigation planning.

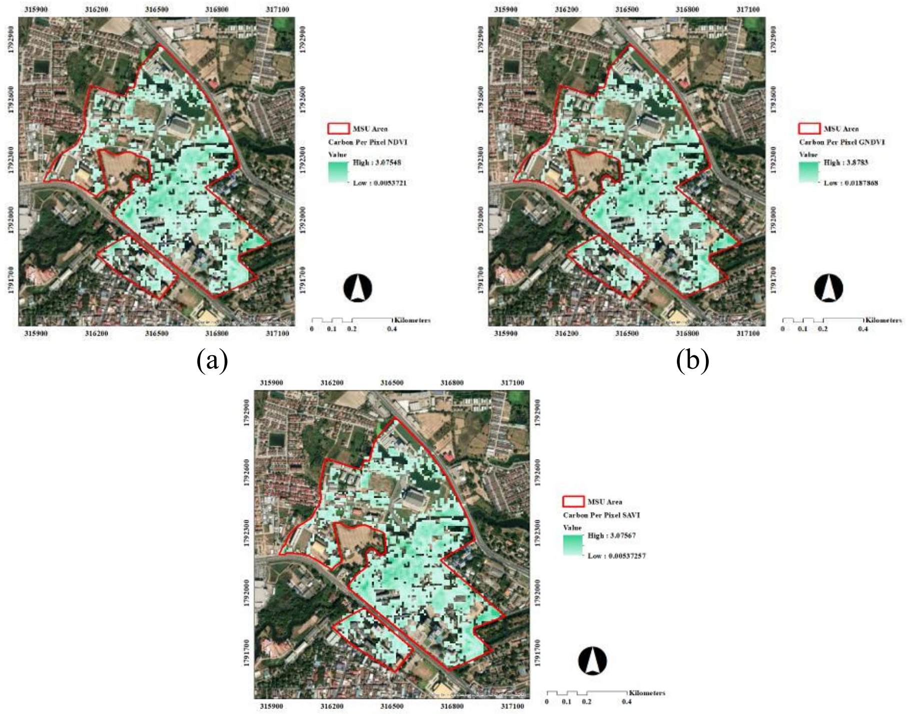

(a) (b)

(c)

Figure 7. Carbon per pixel (a) NDVI, (b) GNDVI, and (c) SAVI

Statistical Accuracy Assessment

In order to assess the accuracy of biomass estimation provided by satellite images, NDVI, GNDVI and SAVI were compared with values measured in field conditions using Root Mean Square Error (RMSE) an d its percentage equivalent (R MSE %). The findings demonstrate a consistent pattern in model behavior. For NDVI, the estimated RMSE was 2.36 t ha^{-1} that means on average the satellite derived estimates are different from field measurement by around 2.36 t ha^{-1} and its relative percentage error was expressed in terms of %RMSE (44.99%). GNDVI conversely, provided the most optimal fit with RMSE value of 1.90 t ha^{-1} and corresponding to lowest RMSE% (36.21%), which means a reasonable approximation between predicted and observed biomass densities. SAVI produced intermediate results with an RMSE of 2.15 t ha^{-1} and an RMSE% of 41.11%, indicating a moderate level of accuracy. Taken together, these findings demonstrate that GNDVI provides the most accurate representation of aboveground biomass density in the study area, outperforming both NDVI and SAVI by reducing estimation error and offering a more reliable basis for biomass modeling. The consistently lower error metrics observed for GNDVI confirm its suitability as the preferred index for aboveground biomass assessment, particularly in heterogeneous landscapes where precision is essential for carbon stock estimation and land management planning.

The statistical accuracy assessment indicated that the GNDVI-based model provided the most optimal performance among all indices, with the lowest RMSE (1.90 t ha^{-1}) and RMSE% (36.21%). This suggests that GNDVI most effectively captures canopy density and chlorophyll characteristics, leading to more reliable aboveground biomass (AGB) predictions in heterogeneous urban landscapes. NDVI and SAVI showed moderate accuracy with RMSE values of 2.36 t ha^{-1} and 2.15 t ha^{-1}, respectively, confirming their usefulness but also their limitations in soil-influenced or mixed-vegetation environments. These findings are consistent with previous studies, indicating that green-band-based indices such as GNDVI perform better in complex canopies. The results reinforce the suitability of exponential regression for representing biomass–cover relationships, with an R^2 of 0.72 showing a strong correlation between fractional vegetation cover (FC) and AGB.

In comparison with other research, Faria *et al.* (2024) reported an RMSE of approximately 15.9% for biomass prediction at the Amazon–Cerrado transition, lower than the RMSE in this study. This difference may be due to their application of Artificial Neural Networks (ANNs), which can capture complex nonlinear relationships between spectral features and biomass. Similarly, Niu *et al.* (2024) achieved an improved coefficient of determination (R^2 = 0.74) by combining UAV and Sentinel-2 datasets, demonstrating the advantage of multi-source integration for improved model robustness. Furthermore, Liu *et al.* (2024b) found that including environmental parameters such as topography significantly enhanced AGB mapping in boreal forests of China (R^2 = 0.75 with reduced error). These comparative observations highlight that while regression-based models remain effective for practical estimation, integrating higher-resolution and multi-source datasets—such as UAV imagery, LiDAR, and environmental parameters—could further improve prediction accuracy. Such hybrid approaches would strengthen spatial–temporal representation of urban ecosystems, supporting precise carbon stock evaluation and sustainable green-space planning.

CONCLUSIONS

This study demonstrated that integrating field-based measurements with
This study demonstrated that integrating field-based measurements with Sentinel-2 satellite imagery provides an effective framework for estimating aboveground biomass (AGB) and carbon stock in urban tree ecosystems. The combination of remote sensing data and allometric modeling produced accurate, spatially explicit estimates essential for sustainable urban forest management. The GNDVI-based model showed the strongest correlation with AGB (R^2=0.72) and yielded the lowest RMSE (1.90 t ha^{-1}), confirming its superior capability for representing vegetation density and chlorophyll content. These findings indicate that GNDVI is the most suitable vegetation index for biomass estimation in heterogeneous urban landscapes, and the developed model can be applied to monitor vegetation dynamics and assess carbon storage capacity in different urban contexts.

By linking remote sensing techniques with ground observations, this study presents a cost-effective and replicable approach for large-scale monitoring of carbon dynamics. The framework can support local authorities and policymakers in formulating urban greening strategies, climate adaptation measures, and the development of carbon credit initiatives aligned with Thailand's Net Zero goals. Furthermore, the approach can be utilized in verification and monitoring processes under carbon credit schemes such as T-VER or VERRA, creating pathways for measurable greenhouse gas reduction. Future research should integrate high-resolution UAV data, LiDAR measurements, and environmental parameters through advanced machine learning algorithms to enhance predictive accuracy and deepen understanding of spatial–temporal variability in urban ecosystems, thereby supporting sustainable urban development and long-term climate resilience.

ACKNOWLEDGEMENTS

This research project is financially supported by Mahasarakham University.

REFERENCES

Aabeyir, R., Adu-Bredu, S., Agyare, W. A., & Amponsah, W. (2020). Allometric models for estimating aboveground biomass in the tropical woodlands of Ghana, West Africa. Forest Ecosystems, 7, 41. https://doi.org/10.1186/s40663-020-00250-3

Angkahad, T., Chokkuea, W., Sangpradid, S., Uttaruk, Y., Viriyasatr, K., & Laosuwan, T. (2025a). The assessment of above ground biomass and carbon sequestration in community forests using UAV technology. Defense Technology Academy Journal, 7(15), R11–R28.

Angkahad, T., Laosuwan, T., Sangpradid, S., Prasertsri, N., Uttaruk, Y., Phoophathong, T., & Nuchthapho, J. (2025b). Developing a drone-based machine learning for spatial modeling and analysis of biomass and carbon sequestration in forest ecosystems. Engineered Science, 35, 1508. https://doi.org/10.30919/es8d1568

Bhebhe, Z. M., Liu, X., Zhang, Z., & Paudyal, D. R. (2025). Estimation of tree diameter at breast height (DBH) and biomass from allometric models using LiDAR data: A case of the Lake Broadwater Forest in southeast Queensland, Australia. Remote Sensing, 17(14), 2523. https://doi.org/10.3390/rs17142523

Castillo, J. A., Apan, A. A., Maraseni, T. N., & Salmo, S. G. III. (2017). Estimation and mapping of above-ground biomass of mangrove forests and their replacement land uses in the Philippines using Sentinel imagery. ISPRS Journal of Photogrammetry and Remote Sensing, 134, 70–85. https://doi.org/10.1016/j.isprsjprs.2017.10.016

Chave, J., Réjou-Méchain, M., Búrquez, A., Chidumayo, E., Colgan, M. S., Delitti, W. B. C., Duque, A., Eid, T., Fearnside, P. M., Goodman, R. C., Henry, M., Martínez-Yrízar, A., Mugasha, W. A., Muller-Landau, H. C., Mencuccini, M., Nelson, B. W., Ngomanda, A., Nogueira, E. M., Ortiz-Malavassi, E., … Vieilledent, G. (2014). Improved allometric models to estimate the aboveground biomass of tropical trees. Global Change Biology, 20(10), 3177–3190. https://doi.org/10.1111/gcb.12629

Dhiman, V., & Kumar, A. (2024). Biomass and carbon stock estimation through remote sensing and field methods of subtropical Himalayan forest under threat due to developmental activities. Environment and Natural Resources Journal, 22(4), 378–393. https://doi.org/10.32526/ennrj/22/20240018

Faria, R. A. P., Ribeiro, E. S., Nascimento, D. C. de S., Silva, A. A., Mello, J. M., & Rios, F. V. (2024). Biomass prediction using Sentinel-2 imagery and an artificial neural network in the Amazon/Cerrado transition region. Forests, 15(9), 1599. https://doi.org/10.3390/f15091599

Gitelson, A. A., Kaufman, Y. J., & Merzlyak, M. N. (1996). Use of a green channel in remote sensing of global vegetation from EOS-MODIS. Remote Sensing of Environment, 58, 289–298. https://doi.org/10.1016/S0034-4257(96)00072-7

Huete, A. R. (1988). A soil-adjusted vegetation index (SAVI). Remote Sensing of Environment, 25(3), 295–309. https://doi.org/10.1016/0034-4257(88)90106-X

Intergovernmental Panel on Climate Change. (2006). 2006 IPCC guidelines for national greenhouse gas inventories. Prepared by the National Greenhouse Gas Inventories Programme. IGES.

Intergovernmental Panel on Climate Change. (2022). The evidence is clear: The time for action is now. We can halve emissions by 2030. IPCC. https://www.ipcc.ch/2022/04/04/ipcc-ar6-wgiii-pressrelease/

Lamenkova, P. (2024). Mapping woodlands in Angola, tropical Africa: calculation of vegetation indices from remote sensing data. Agriculture and Forestry, 70 (3): 185-202. https://doi.org/10.17707/AgricultForest.70.3.13

Laosuwan, T., Plybour, C., Rotjanakusol, T. (2023). Inspection of burning areas caused by forest fire in doi suthep-pui national park through data obtained from Landsat 8 satellite and normalized burn ratio. Agriculture and Forestry, 69(3), 81-95. https://doi.org/10.17707/AgricultForest.69.3.06

Laosuwan, T., Rotjanakusol, T., Chokkuea, W., Singharath, M., & Itsarawisut, J. (2025b). Creation of technique for assessing above ground biomass and carbon sequestration using unmanned aerial vehicles. Geographia Technica, 20(2), 65–78. https://doi.org/10.21163/GT_2025.202.05

Laosuwan, T., Uttaruk, Y., Nakapan, S., Itsarawisut, J., & Plybour, C. (2025a). Evaluation of tree biomass and carbon sequestration through remote sensing and field methods. Geographia Technica, 20(1), 33–43. https://doi.org/10.21163/GT_2025.201.04

Liu, P., Zhang, Y., Hu, T., Zhai, D., & Zhao, F. (2024a). Combining Sentinel-2 and diverse environmental data to map aboveground biomass in China’s boreal forests. Scientific Reports, 14, 15423. https://doi.org/10.1038/s41598-024-78615-9

Liu, X., Dong, L., Li, S., Li, Z., Wang, Y., Mao, Z., *et al.* (2024b). Improving AGB estimations by integrating tree height and crown radius from multisource remote sensing. PLOS ONE, 19(10), e0311642. https://doi.org/10.1371/journal.pone.0311642

Muluneh, M. G. (2021). Impact of climate change on biodiversity and food security: A global perspective—A review article. Agriculture & Food Security, 10, 36. https://doi.org/10.1186/s40066-021-00327-4

Ngomanda, A., Engone Obiang, N. L., Lebamba, J., Moundounga Mavouroulou, Q., Gomat, H., Mankou, G. S., Loumeto, J., Midoko Iponga, D., Kossi Ditsouga, F., & Zinga Koumba, R. (2014). Site-specific versus pantropical allometric equations: Which option to estimate the biomass of a moist Central African forest? Forest Ecology and Management, 312, 1–9. https://doi.org/10.1016/j.foreco.2013.10.029

Niu, L., Liu, X., Zhang, H., Zhang, Y., Chen, L., & Wang, J. (2024). Estimation of coastal wetland vegetation aboveground biomass by integrating UAV and satellite remote sensing data. Remote Sensing, 16(15), 2760. https://doi.org/10.3390/rs16152760

Ofremu, G. O., Raimi, B. Y., Yusuf, S. O., Dziwornu, B. A., Nnabuife, S. G., Eze, A. M., & Nnajiofor, C. A. (2025). Exploring the relationship between climate change, air pollutants and human health: Impacts, adaptation, and mitigation strategies. Green Energy and Resources, 3(2), 100074. https://doi.org/10.1016/j.gerr.2024.100074

Ogawa, H., Yoda, K., Ogino, K. and Kira, T. (1965). Comparative ecological studies on three main types of forest vegetation in Thailand II. Plant biomass. Natural and life in Southeast Asia, 4, 49-80.

Rahim, N. H., Abdul Razak, S., Chang, X., Saun, F. C., Nauman Khan, M., Hamzah, S. N., Rohman, F., Ali, B., Kaplan, A., Iqbal, M., Bozhuyuk, M. R., & Ercisli, S. (2024). Ecosystem services by urban forest (UF) towards climate change adaptation: A review. Polish Journal of Environmental Studies, 33(4), 3503–3513. https://doi.org/10.15244/pjoes/177147

Roy, D. P., Kovalskyy, V., Zhang, H. K., Vermote, E. F., Yan, L., Kumar, S. S., & Egorov, A. (2016). Characterization of Landsat-7 to Landsat-8 reflective wavelength and normalized difference vegetation index continuity. Remote Sensing of Environment, 185, 57–70. https://doi.org/10.1016/j.rse.2015.12.024

Saatchi, S., Xu, L., Shapiro, A., Meyer, V., Ferraz, A., Yang, Y., Bastin, J. F., Clark, D. B., Garvin, C., Harris, N. L., Houghton, R. A., Kearsley, E., Lindsell, J. A., Mitchard, E. T. A., Morel, A., Næsset, E., Nelson, B., Pang, Y., Pearson, T. R. H., … Yu, Y. (2021). Detecting vulnerability of humid tropical forests to multiple stressors. Global Change Biology, 27(9), 1817–1833. https://doi.org/10.1111/gcb.15526

Saengpradit, P., Sangpradid, S., & Laosuwan, T. (2024). Estimation of aboveground biomass using hybrid machine learning based on satellite imagery. International Journal on Technical and Physical Problems of Engineering, 16(4), 7–13.

Semosa, P. D. (2025). The Impact of Climate Change on the Agricultural Sector in SADC Countries. Sustainability, 17(11), 5177. https://doi.org/10.3390/su17115177

Tucker, C. J. (1979). Red and photographic infrared linear combinations for monitoring vegetation. Remote Sensing of Environment, 8, 127–150. https://doi.org/10.1016/0034-4257(79)90013-0

Uttaruk, Y., & Laosuwan, T. (2020). Methods of estimation for aboveground carbon stock in Nongbua-Nonmee Community Forest, Maha Sarakham Province, Thailand. Agriculture and Forestry, 66(3), 183–195. https://doi.org/10.17707/AgricultForest.66.3.15

Uttaruk, Y., Laosuwan, T., Sangpradid, S., Butthep, C., Rotjanakusol, T., Sittiwong, W., & Nilrit, S. (2024). Thailand's urban forestry programs are assisted by calculations of their ecological properties and economic values. Land, 13(9), 1440. https://doi.org/10.3390/land13091440

Van Breugel, M., Ransijn, J., Craven, D., Bongers, F., & Hall, J. S. (2011). Estimating carbon stock in secondary forests: Decisions and uncertainties associated with allometric biomass models. Forest Ecology and Management, 262(9), 1648–1657. https://doi.org/10.1016/j.foreco.2011.07.018

Vattanavongsiri, W., Sangpradid, S., Chokkuea, W., & Laosuwan, T. (2023). Estimation of above-ground carbon sequestration in the national reserved forest using vegetation indices and gradient boosting machine learning. International Journal on Technical and Physical Problems of Engineering, 16(3), 361–366.

Wavrek, M. T., Carr, E., Jean-Philippe, S., & McKinney, M. L. (2023). Drone remote sensing in urban forest management: A case study. Urban Forestry & Urban Greening, 86, 127978. https://doi.org/10.1016/j.ufug.2023.127978

Wolf, K. L., Lam, S. T., McKeen, J. K., Richardson, G. R. A., van den Bosch, M., & Bardekjian, A. C. (2020). Urban trees and human health: A scoping review. International Journal of Environmental Research and Public Health, 17(12), 4371. https://doi.org/10.3390/ijerph17124371

Xiao, J., Chen, L., Zhang, T., Li, L., Yu, Z., Wu, R., Bai, L., Xiao, J., & Chen, L. (2022). Identification of urban green space types and estimation of above-ground biomass using Sentinel-1 and Sentinel-2 data. Forests, 13(7), 1077. https://doi.org/10.3390/f13071077